Journal of Loss Prevention in the Process Industries 84 (2023) 105123

Contents lists available at ScienceDirect

Journal of Loss Prevention in the Process Industries

journal homepage: www.elsevier.com/locate/jlp

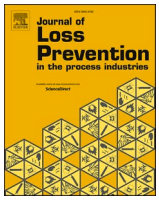

On the effectiveness of mitigation strategies for cryogenic applications

Paolo Mocellin [a], Gianmaria Pio [b,*], Mattia Carboni [a], Francesco Pilo [c], Chiara Vianello [a,d], Ernesto Salzano [b]

[a] Dipartimento di Ingegneria Industriale, Università degli Studi di Padova, Via Marzolo 9, 35131, Padova, Italy
[b] Dipartimento di Ingegneria Civile, Chimica, Ambientale e dei Materiali, Università degli studi di Bologna, Via Terracini 28, 40131, Bologna, Italy
[c] Corpo Nazionale dei Vigili del Fuoco Comando Venezia, Via Motorizzazione 7, 37100, Venezia, Italy
[d] Dipartimento di Ingegneria Civile, Edile e Ambientale, Via Marzolo 9, 35131, Padova, Italy

ARTICLE INFO

Keywords:
Cryogenic fuels
Liquefied natural gas
Pool fire
Water-based mitigation systems
Flare
Safety

ABSTRACT

The need for sustainable energy sources, as well as the current energetic crisis involving the majority of markets, has promoted the use of cryogenic liquefaction for the transportation and storage of natural gas (i.e., LNG). To guarantee the development of a robust and safe infrastructure, a complete understanding of the main phenomena occurring at low temperatures is paramount. In this sense, the largest grey areas are the characterization of the combustion at low-initial temperature and the interactions between water and cryogenic liquid. For these reasons, this work presents an experimental campaign on the possible mitigation strategies for the mitigation of consequences related to the accidental release of LNG. Particular emphasis was posed on the direct and indirect effects of water on cryogenic pool fire. The former resulted in a significant increase in the dimensions of fire (~+50%) and burning rate (~300%) with respect to the case with no direct contact between water and LNG, whereas the latter generated an abrupt decrease in the measured temperatures (<100 °C). The use of an emergency flare to empty an LNG tank was tested, as well. The spatial distribution of temperature was monitored along with the time to guarantee the safe operability of this equipment in the case of LNG combustion. The explanations for the observed phenomena and trends were provided, allowing for the development of safe procedures for the emergency response related to cryogenic fuels.

1. Introduction

The energy transition we are currently experiencing to meet the international requirements in the field of environmental sustainability promoted the implementation of innovative solutions for energy production on a large scale. The research and development programs associated with this trend have led to the introduction of cryogenically liquefied fuels, such as liquefied natural gas (LNG), as a viable alternative in the short and medium terms (Scurlock, 2015). Indeed, the use of LNG allows for the retrofit of existing facilities currently using natural gas as a fuel (Withers et al., 2014). Besides, the acquired knowledge on the subject can promote the use of similar conditions for cleaner energy vectors in a long-term perspective, namely paving the way to the realization of infrastructures for the use of liquid hydrogen (Klebanoff et al., 2017; Mocellin et al., 2018).

Although LNG has shown an excellent safety record due to elevated standards in risk management (Mokhatab et al., 2014), some concerns still exist about its use on an industrial scale. It is worth mentioning the recent effort performed by the scientific community in providing numerical tools and experimental databases suitable for the characterization of accidental scenarios resulting from an accidental spill of LNG (Qi et al., 2010)(Pio et al., 2019a) (Gerbec et al., 2021). In this sense, the pool fire represents the most critical scenario to be analyzed because of its capability to generate physical vectors potentially triggering cascading events (Pio et al., 2019b). On the one hand, several studies have focused on quantifying the main properties of a large-scale LNG pool fire, as reported in detail within the review proposed by Luketa-Hanlin, 2006. On the other hand, fewer data are available once the scale is reduced to a credible release size for bunkering operations (Jeong et al., 2020) (Carboni et al., 2022a; Nguyen et al., 2022). Besides, identifying effective mitigation (extinguishing) solutions suitable for fire generated by cryogenic fuels is an essential step to guaranteeing their safe use on an extensive basis (Carboni et al., 2022b; George et al., 2019). Indeed, firefighting represents one of the most significant steps of

* Corresponding author.
E-mail address: gianmaria.pio@unibo.it (G. Pio).

https://doi.org/10.1016/j.jlp.2023.105123
Received 24 January 2023; Received in revised form 16 May 2023; Accepted 10 June 2023
Available online 17 June 2023

the emergency response plans for bunkering operations (European Maritime Safety Agency, 2017). Nevertheless, a dearth of experimental data and numerical investigations on the effectiveness of mitigation systems and procedures can be observed in the current literature despite the maturity of the technological systems potentially involved (Kang et al., 2022). In this regard, standard procedures for mitigation, i.e., water-based systems, N_2 or CO_2, or solid suppression (application of expanding foams, powders, or fibrous solids) (Carson and Mumford, 2013), can be considered in the first instance. Nevertheless, when cryogenic systems are of concern, the ultra-low temperature of the pool can affect the effectiveness of these approaches. Indeed, the flame expansion due to the application of water mist on a pool fire is typically affected by the fuel type, the water momentum and direction (Xiao et al., 2011). Besides, the contact between large water particles and liquid pools increases the intrinsic mixing among them, enhancing the heat transfer coefficient and, thus, the evaporation rate and the severity of pool fire (Xiao et al., 2011). However, relevant uses for water in fighting liquefied gas fires can still be possible. Indeed, water can be used to cool surfaces exposed to heat radiation or directly engulfed by the fire to avoid domino effects on other equipment containing hazardous materials, such as tanks or critical structural components (water deluge) (Vianello et al., 2020). Besides, a water curtain can be implemented as a diffused spray to limit the thermal effect of radiation on the far field (Sun et al., 2017). This strategy is paramount to realize a safe pattern for evacuation purposes, especially in highly congested areas such as bunkering terminals (Kim et al., 2021). Conversely, if an LNG tank is exposed to fire or damaged, movable flare systems can be considered as a solution to avoid cascading events. In contrast with the typical applications of this strategy for traditional fuels, the use of LNG requires particular attention to evaluate the combustion at low initial temperatures (Pio and Salzano, 2021).

For these reasons, field tests were designed and carried out in this work to characterize the effectiveness of the available strategies in firefighting an LNG pool fire. More specifically, either the direct or the indirect use of water on pool fire will be discussed, as well as the spread of LNG on wet surfaces and the use of a movable flare for an emergency will be tested. A mechanism accounting for physical and kinetic aspects at a microscopic level to describe the observed phenomena was introduced. Besides, the collected measurements can be also considered as a database for the realization and validation of dedicated models suitable for the safety characterization of cryogenic applications.

2. Materials and methods

The experimental campaign conducted in this work was performed at the Nuclear Biological Chemical and Radiological (NBCR) camp of the Italian National Fire and Rescue Service, and it was focused on the characterization of thermal aspects (e.g., temperature profiles and fluxes) generated by mitigated LNG releases. To this aim, several on-field experiments were carried out using type-K thermocouples with an acquisition frequency of 0.5 Hz and a FLIR thermal imaging camera (model T1010) with a frame rate of 30 Hz. The composition adopted throughout the whole set of tests can be expressed in terms of volumetric fraction as follow: $CH_4 = 89.48\%$, $C_2H_6 = 8.76\%$, $C_3H_8 = 1.16\%$, $N_2 = 0.50\%$, and $C_4H_{10} < 0.1\%$. At first, the effects of either direct (i.e., fire hose) or indirect (i.e., water curtain) application of water were tested on an LNG pool. These tests were referred to as Test A and Test B, respectively. In both cases, after a preliminary phase in the absence of water to stabilize an unmitigated pool fire, a volumetric flow rate of 150 l min^{-1} was employed to evaluate its effect on the resulting scenario. The fire hose was sprayed directly on the pool, whereas the water curtain was located on the ground at a distance of 0.70 m (x-direction) from the origin after thermocouple H5, as shown in Fig. 1. The water curtain produced a water screen of 7 m of the radius with an initial particle velocity of 3 m s^{-1}. The abovementioned tests were performed using a steel rectangular-shaped drip tray of 0.75 × 0.48 × 0.01 m. The liquid

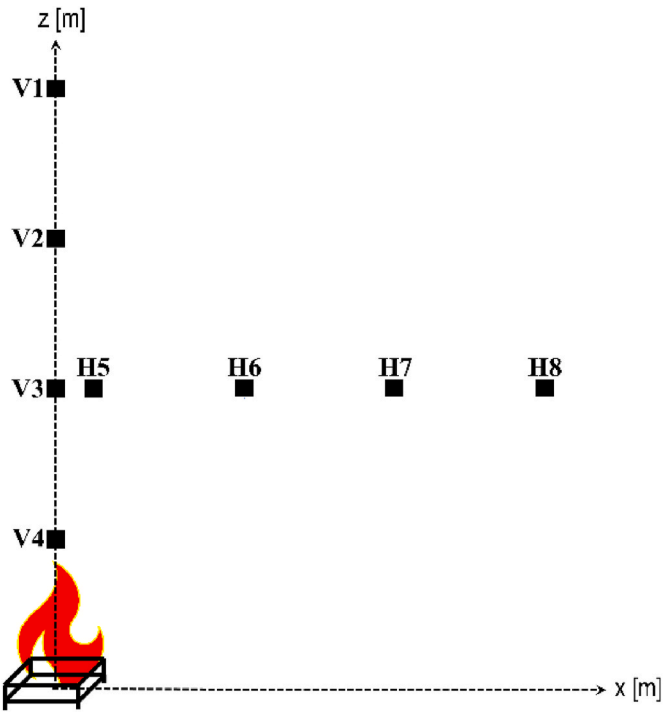

Fig. 1. Experimental setup employed for pool fire tests. The squares represent the type K thermocouples. The spacing is 1 m in the x and y direction. H5 is located 0.375 m from the y-axis.

mass, along with the time of the test, was measured through load cells with a resolution of 20 g and a sampling frequency of 0.1 Hz. Then, the possible overfill with the consequent spread of LNG on a wet surface was realized and characterized (Test C). Eventually, Test D was conducted to analyze the temperature field produced from a movable flare usually employed in emergency operations since this equipment is typically used when the emergency discharging of tanks is required. The flare comprises six combustion points, one of which is positioned at the centre. A 4 mm diameter nozzle forms each combustion point. The peripheral combustion points are located at a height of 1.90 m above the ground, while the central one is at 2.20 m (Fig. 2 and S6). A 1″ AISI 304 pipe connects the flare to the LNG tank. The temperature field developed during the test was measured by keeping the distance between thermocouples constant with respect to the previously described tests.

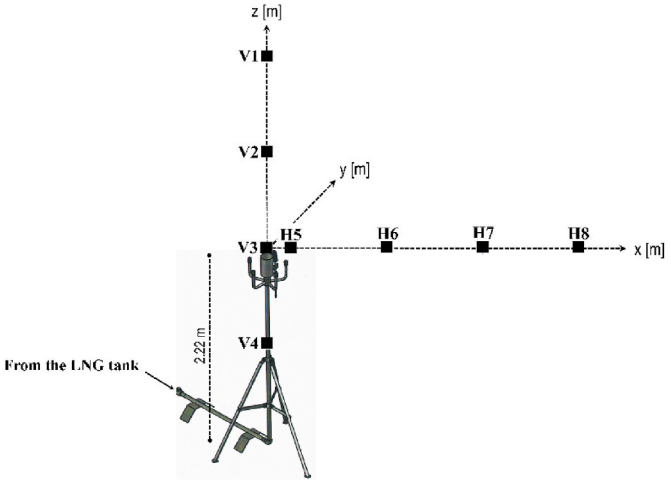

Fig. 2. Experimental setup employed for flare fire test. Localization of type K thermocouples.

However, in this case, the origin of the axis was posed on top of the central combustion point (Fig. 2 and Table 1). Fig. 2 and S6 show the geometrical details of the flare, whereas a summary of experiments conducted in this work is presented in Table 2.

Test D was intended to reproduce credible conditions in which an LNG tank needs to be emptied, thus two different conditions can be distinguished:

1. Constant mass flow rate: At the beginning of the test (up to 05:00 min), only the liquid phase was supplied, and the flare mass flow rate $\dot{m}''_{flare}$ was constantly equal to 350 kg h^{-1} and the pressure P to 7.5 bar;
2. Decreasing mass flow rate: in the second part of the test, i.e., when two phases were fed to the burner, P varied with time (Fig. 3) and, consequently, $\dot{m}''_{flare}$ changed along with the time. In this case, an average value $\overline{\dot{m}''_{flare}}$ of 61 kg h^{-1} was obtained.

Considering the nature of the experimental campaign (i.e., on-field tests), it should be considered that boundary conditions related to ambient temperature, humidity and wind velocity can slightly change with each test. In this regard, the experimental campaign was arranged to work under limited weather excursions. Besides, the atmospheric conditions were monitored along with the test. For the sake of simplicity, only the average conditions are reported in Table 3 in terms of ambient temperature (T_a), humidity (H), wind velocity (u_w) and wind direction (d_w).

3. Results and discussion

This section discusses the results of tests performed in this work, under the conditions reported in Table 2. Section 3.1 illustrates the results of the experiments of LNG pool fires mitigated with water sprinklers or curtains (Tests A and B); Section 3.2 focuses on the LNG spreading on wet concrete (Test C), and Section 3.3 outlines the results obtained using the movable emergency flare (Test D).

3.1. Direct and indirect use of water systems on LNG pool fires (Test A and B)

Fig. 4 presents the evolution of flame geometry with time during the direct application of water-based mitigation systems. In the first panel (Frame a), the water comes in contact with the liquid pool. An ephemeral reduction of flame geometry can be observed in the second panel (Frame b) because of the interactions between water and flame. This aspect suggests the potentiality of the indirect application of water-based mitigation systems that will be analyzed later in this work. In the third panel (Frame c) water system was shut down to restore the initial conditions. Then, water was newly added, as testified by Frame d. At this stage, flame dimensions were considerably increased, and an acoustic wave associated with a rapid phase transition (RPT) (Carboni et al., 2021) was recorded. In addition, when the water was sprayed, the flame height (H_f) increased to 51%, and the flame diameter (D_f) more than doubled. These variations can be attributed to the enhanced heat transfer between the liquid pool and the atmosphere (Incropera et al., 2007), producing a larger amount of vapour available for combustion.

Table 1
Position of thermocouples adopted for the characterization of temperature distribution from a flare fire test expressed in x, y and z coordinates considering the centre of the drip tray as the origin.

	V1	V2	V3	V4	H5	H6	H7	H8
x [m]	0	0	0	0	0.375	1.375	2.375	3.375
y [m]	0	0	0	0	0	0	0	0
z [m]	2	1	0	−1	0	0	0	0

Table 2
Summary of the main features of the experimental tests performed.

Test	Scenario	Initial mass [kg]	Description
Test A	Pool fire	16.50	Water directly used on the fire (fire hose)
Test B	Pool fire	19.50	Water indirectly used on the fire (water curtain)
Test C	Pool fire	22.70	LNG spread on wet concrete
Test D	Flare		Flare test

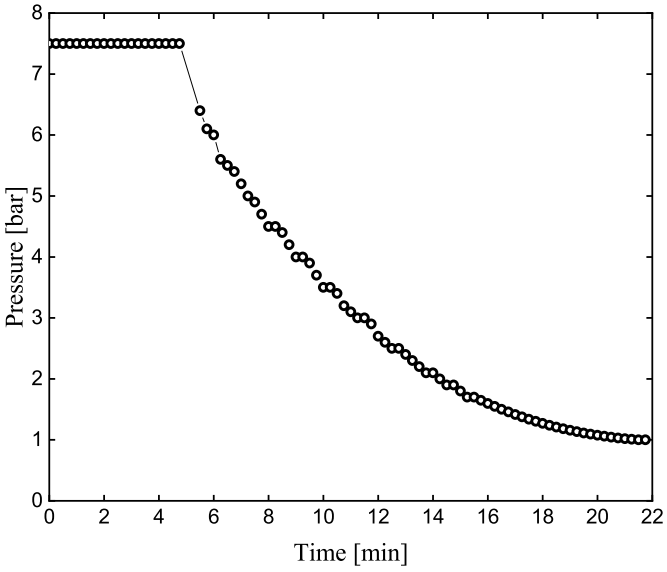

Fig. 3. Time evolution of the tank pressure profile as measured during Test D.

Table 3
Summary of the average values of the atmospheric conditions registered during each test. Please consider the following nomenclature: ambient temperature (T_a), humidity (H), wind velocity (u_w) and wind direction (d_w).

Test	T_a [°C]	H [%]	u_w [m s^{-1}]	d_w [°]
Test A	3.7	44	0.5	322
Test B	7.0	32	1.0	286
Test C	7.2	31	1.7	22
Test D	6.6	32	0.7	96

Indeed, the average $\dot{m}''$ in the absence of water was calculated as 0.042 kg s^{-1} m^{-2}. This value is in line with data reported by Babrauskas (1983) for pool diameters smaller than 2 m, whereas it is significantly smaller than the homologous data reported by large-scale tests (Esteves and Reis Parise, 2013) which are typically considered for the consequence analysis. This discrepancy implies that, once medium-scale releases are of concern, more accurate values of mass burning rate may be adopted. Conversely, the direct contact of water with LNG makes the mass burning rate triple (i.e., $\dot{m}'' = 0.144$ kg s^{-1} m^{-2}), demonstrating the inadequacy of direct use of water on LNG pool fire as an extinguishing agent. In addition, starting from Frames e and f of Fig. 4, it is possible to see a large white cloud from the pool. Considering the refracting indexes of the species involved in the analyzed scenario, the abovementioned cloud can be associated with the presence of a local pocket rich in water vapour (Carboni et al., 2022c). Indeed, the white cloud is weakly affected by wind speed, as demonstrated by the observed tilt angle. Besides, the presence of cold fuel vapours can be excluded by the absence of a gravity-dominated phase, typically associated with the release of cryogenic fuels (Koopman and Ermak, 2007). On the contrary, the wind significantly affects burned products, although they have a

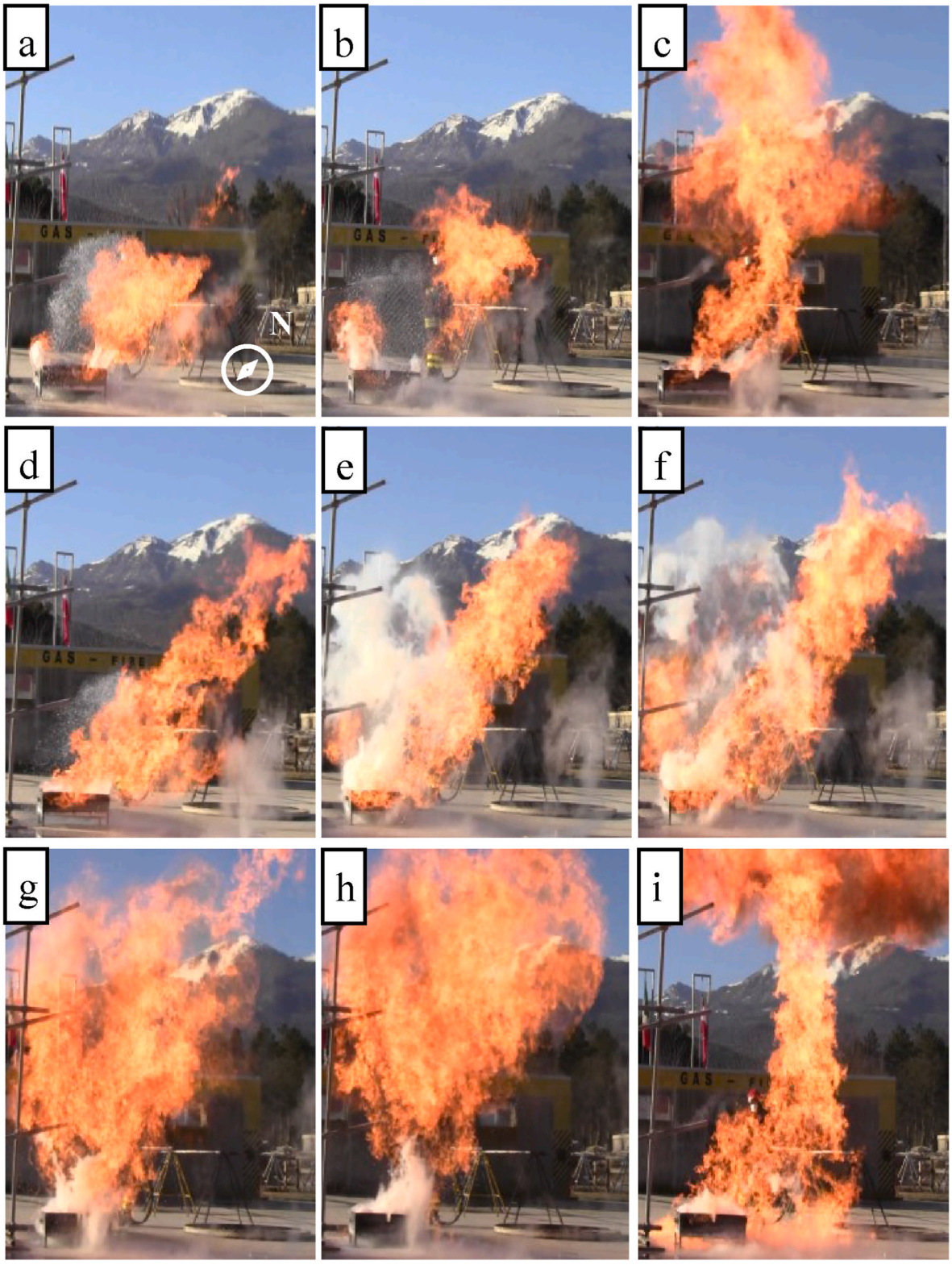

Fig. 4. Time evolution of the flame geometry as obtained during Test A.

larger molecular weight. This discrepancy can be attributed to their average temperature. Indeed, the vapour cloud can be characterized by a maximum temperature equal to the dew point (T_{dew}), as reported in Equation (1) (Bosen, 1958).

$$T_{dew} = \left(\frac{H}{100}\right)^{\frac{1}{8}} (112 + 0.9\, T_a) + 0.1\, T_a - 112 \quad (1)$$

Starting from the equation above, a temperature approximately of −7.5 °C can be expected for the vapour cloud, whereas a diffusive flame of methane can reach a temperature considerably larger than 1000 °C (Lin et al., 2018). Based on these observations, it is possible to infer that the influence of water on termination reactions, mentioned as a possible indirect role, could be neglected if the typical size and structure of low-initial temperature flames are considered (Pio et al., 2019a).

Indeed, the added water can interact with the flame only in the proximity of the pool, where the low-temperature pocket associated with the fuel activation is expected. Under these circumstances, the direct role of water and physical dilution can be intended as the most prominent factors impacting the LNG pool fire from a chemical point of view. Indeed, the presence of water can hinder the formation of methyl radicals (CH_3) through the reaction $CH_4 + OH \leftrightharpoons CH_3 + H_2O$ as well as the formation of HCO via the reaction $HCO + (M) \leftrightharpoons H + H_2O$, modifying a key step in the oxidative decomposition path of methane (Hashemi et al., 2016), especially at low temperatures (Pio and Salzano, 2018). In this light, dedicated investigations on the kinetic interactions between small radicals and water at low temperatures are suggested.

From a physical point of view, the difference between the density of water in liquid and vapour phases, together with the presence of steam in the proximity of the pool, suggests that the vaporization of water is the cause of the observed rapid phase transition, which breaks down the film boiling and produces the acoustic wave following the classical theory reported by Aursand and Hammer for the case of LNG spill on water (Aursand and Hammer, 2018). Indeed, the generated wave disaggregates the flame from the pool (Frames g and h). Hence, a more intense liquid (water) - liquid (LNG) mixing can be observed. These conditions make the system prone to an overflow of part of the fuel from the drip tray (Frame i), enlarging the area involved in the fire. For these reasons, a specific focus on the spread of LNG on wet concrete will be provided once Test C will be analyzed. For a short time, H_f values higher than 4 m were registered.

Other than the size of the visible flame, the direct introduction of water to an LNG pool fire leads to significant modifications in the measured temperatures, as shown in Fig. 5. Indeed, an abrupt increase in measured temperature was observed, affecting the level of thermal radiation associated with the maximum recorded temperature. It is worth noting that although this value overcomes 5 kW m^{-2}, the obtained thermal radiation is still lower than the threshold values typically considered as per escalation (Cozzani et al., 2006).

Fig. 6 reports LNG pool fire snapshots in the absence (a) and presence (b) of a water curtain (Test B). A quantity of 19.6 kg of LNG was spilt into the drip tray, and the resulting pool fire was analyzed. The test lasted 12:30 min. At about 8:00 min, a water curtain placed in between *H5* and *H6* was activated. In this case, a metal bulkhead was placed to limit the effect of wind on the flame. No effects of water on the flame structure were observed during this test.

The measured temperature (Fig. 7) reached the maximum value of 780 °C in *V4*, and, along with the horizontal profile, an increase of 50 °C was registered with respect to the homologous measurements from previous tests up to 2.35 m far from the pool centre (i.e., thermocouple *H7*). IR images for Test B were reported in supplementary materials exclusively (Fig. S2). Once the water curtain system was activated, the temperatures were drastically reduced. Indeed, the average and the maximum temperatures registered by the thermocouples after the activation of the water curtain were reduced by 20–57% and 5–86%, respectively (Table 4).

The effectiveness of water spray curtains to mitigate the consequences related to the accidental release of LNG has been also demonstrated by the experimental campaign devoted to the characterization of non-ignited scenarios reported by (Rana et al., 2008).

3.2. LNG spreading on wet concrete (Test C)

The direct use of water as a mitigation medium for pool fires caused by LNG can lead to local overfill of flammable substances. Hence, a later stage characterized by LNG spread on a wet surface can be realized. In this sense, the time evolution of Test C is presented in Fig. 8. In this case, a spill of LNG from the initial tank was produced (Frame a). It is important to notice that a rapid spread of LNG on the wet ground was detected (Frame b). Besides, the formation of ice was observed (Frames a, b, and c), following the theoretical studies on the release of LNG on a shallow-water surface published by Vesovic (2007) (Vesovic, 2007). The velocity of the visible ice particles moving on the wet ground was reconstructed, showing a maximum value of 0.82 ms^{-1}. The spread of LNG on the wet surface enlarges the area where flammable vapours can be obtained. Hence, the initial pool fire can act as an ignition source, causing a flame propagation similar to a late flash fire (Frames d and e). The occurrence of this scenario leads to a fast consumption of most of the flammable substances spilt on the ground, which turns out in localized pockets of fuels. Eventually, the powder fire extinguisher employed to contain the fire (Frame f) achieved excellent results in re-establishing the initial conditions.

3.3. Movable emergency flare (Test D)

The flare test was performed to investigate the temperature field resulting from a movable flare used for the emergency discharging of tanks. The geometrical features of the flame observed in Test D were expressed in terms of liftoff height (H_l), flame height (H_f), flame length (L_f), flame area (A_f), flame diameter (D_f), and tilt angle (δ), as reported in Fig. 9. For the sake of conciseness, a summary of the measured properties is given in Table 5, whereas the evolution along the time of these properties is reported in the supplementary materials (Fig. S7). A maximum height $H_f + H_l$ of 3.08 m was registered. As for the other parameters, H_f is considerably reduced in the gas-liquid phase. Indeed, the transition between the phases is easily recognizable in all the measured trends with respect to time. In this light, the maximum and the

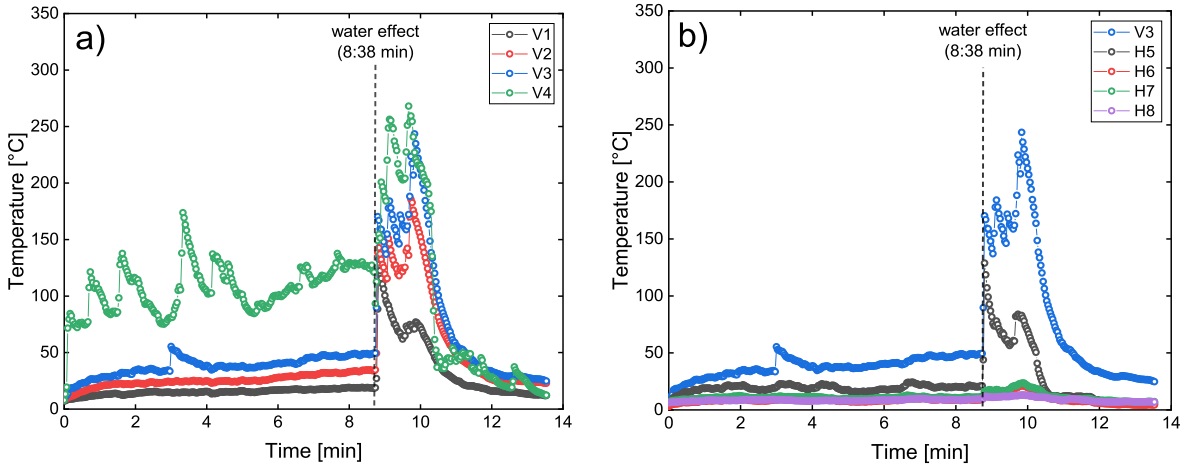

Fig. 5. Time evolution of vertical a) and horizontal b) temperature profiles as measured during Test A.

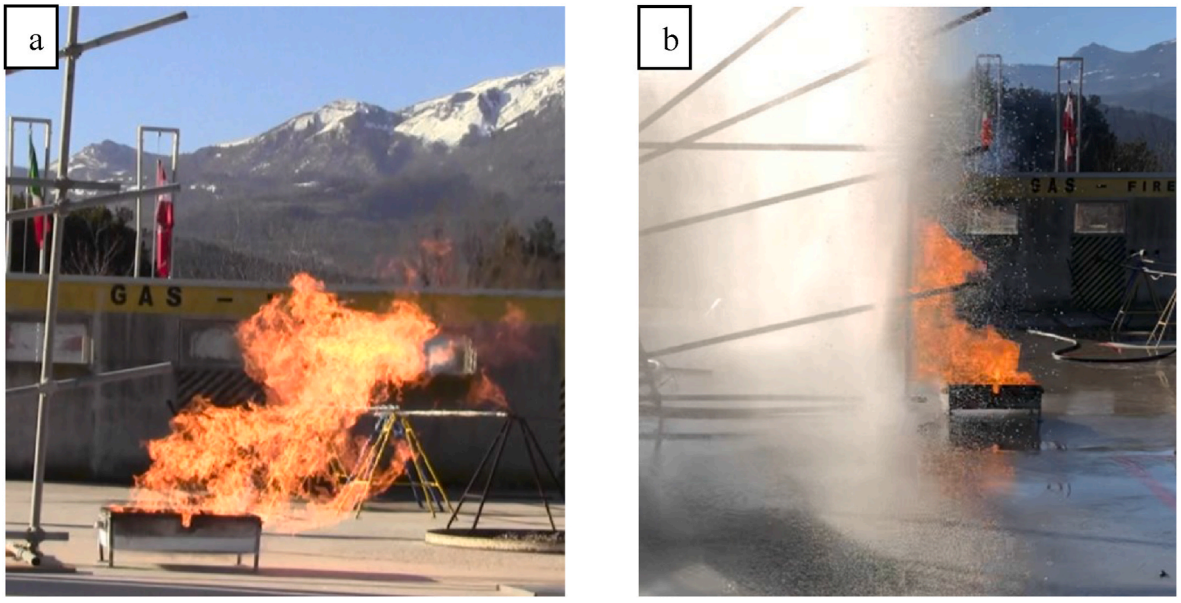

Fig. 6. Time evolution of the flame geometry as obtained during Test B. a) without water curtain; b) with water curtain.

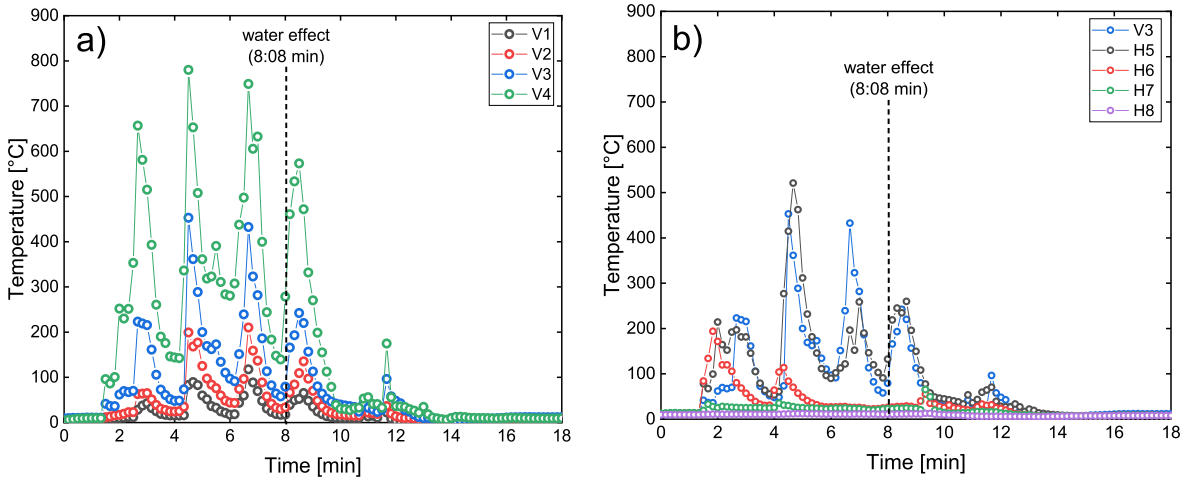

Fig. 7. Time evolution of vertical a) and horizontal b) temperature profiles as measured during Test B.

Table 4
Evaluation of the effect of the water curtain employed in Test B. The maximum (Max) and the average for time (Average) temperature are reported before and after the activation of the water curtain (AWC). The arrangement of thermocouples is provided in Fig. 1.

Value	AWC	Temperature [°C] (Variation [%])							
		V1	V2	V3	V4	H5	H6	H7	H8
Average	No	34	65	145	338	164	57	25	11
	Yes	20 (−40)	38 (−42)	74 (−49)	147 (−57)	86 (−48)	27 (−52)	20 (−19)	9 (−20)
Max	No	118	210	453	780	521	194	35	12
	Yes	65 (−44)	135 (−36)	242 (−47)	573 (−27)	260 (−50)	55 (−72)	65 (−86)	13 (−5)

minimum values reported in Table 5 can be associated with the constant flow rate and decreasing flow rate phases, respectively. An average H_l of 0.44 m was registered under the constant mass flow rate regime, representing ~16% of H_f on average, suggesting the non-negligible contribution made by this part when considering the total height reached by the flame.

In addition, the temperature distribution developed during the test was measured (Fig. 10) employing the thermocouples located as schematized in Fig. 2. As it is possible to note, the maximum temperature reached is notably higher than the one obtained in the pool fire tests. Indeed, a value of ~1070 °C was retrieved 1 m above the combustor point (thermocouple V2, Fig. 2) during the liquid phase. In addition, a drastic decrease in the temperature field is registered after 09:00 min, namely when the pressure inside the tank reaches 4 bar. Regarding the horizontal profile at the height of 2 m, very low-temperature values were achieved, indicating an intrinsic safety and operability of the adopted flare.

Although different experiments under the same conditions were not

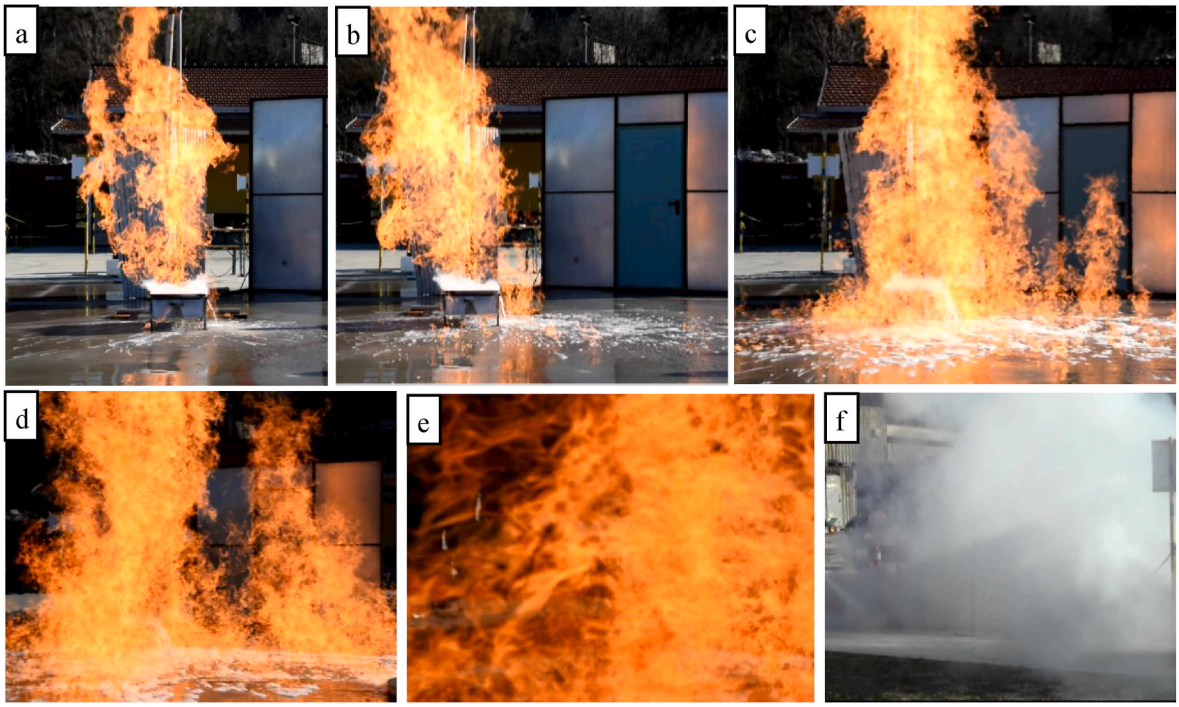

Fig. 8. Time evolution of the flame geometry as obtained during Test C.

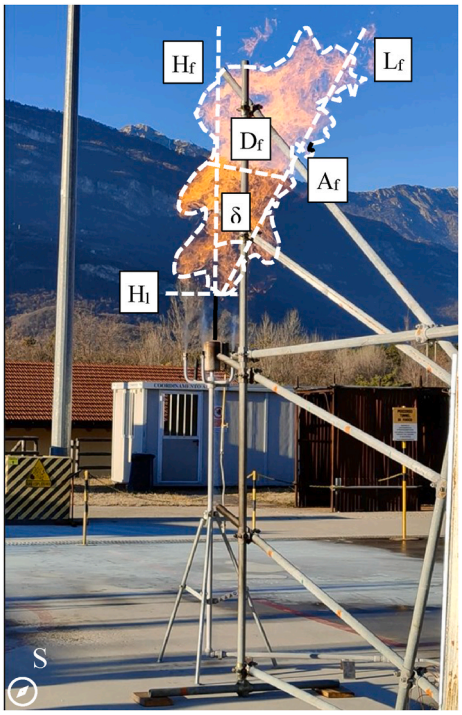

Fig. 9. Schematic representation of the main geometrical features of the flame observed in Test D. Please consider the following nomenclature: liftoff height (H_l), flame height (H_f), flame length (L_f), flame area (A_f), flame diameter (D_f), and tilt angle (δ).

performed in this work, it is important to notice that several aspects can be considered to guarantee the robustness of the collected data. Indeed, redundancies in the measuring system were installed, a steady state is achieved, and a pool fire of LNG was realized as the first step for all tests, showing similar results.

Table 5
Geometrical characteristics of the flame produced by the flare analyzed during Test D.

Phase		H_f [m]	D_f [m]	A_f [m^2]	H_l [m]	T [°C] (# thermocouple)
Liquid	Max	2.74	2.03	2.04	0.72	1069 (V2)
	Average	1.96	1.31	1.41	0.44	–
	Min	1.34	0.91	0.96	0.31	–
Gas-liquid	Max	1.19	0.95	1.10	0.53	882 (V2)
	Average	0.62	0.57	0.21	0.25	–
	Min	0.20	0.25	0.03	0.10	–

4. Conclusions

An experimental campaign devoted to the characterization of the effectiveness of some of the most common mitigation systems for LNG pool fires was conducted and presented in this work. Besides, the effect of low temperature on the combustion mechanism of natural gas was discussed on the basis of newly collected experimental data. It was observed that water sprayed directly on the pool worsened the scenario and could double the flame diameter, increasing the flame height by more the 50% and enhancing the burning rate by a factor of 3. Moreover, an RPT phenomenon was experienced although the limited quantities of liquid involved in this test. Once a water curtain is used in the vicinity of the pool, a significant reduction of measured temperatures is obtained. The consequences of an LNG spill on a wet surface were also evaluated. Based on the experimental data collected in this work, the direct and indirect chemical and physical roles of water in the pool fire of LNG were individuated and discussed. A phenomenological-based mechanism accounting for microkinetic aspects was proposed in this work to provide a possible explanation of the observed trends. An emergency flare system able to burn more than 46 kg of LNG in 22 min was tested, as well. During its operation, a temperature up to 1070 °C was registered. Nevertheless, maximum temperatures lower than 75 °C were measured at a horizontal distance ≥2 m from the flare at the height of 2.0 m above the ground, suggesting an intrinsic safety for people and equipment close to the flare. The robustness and safety of the procedure

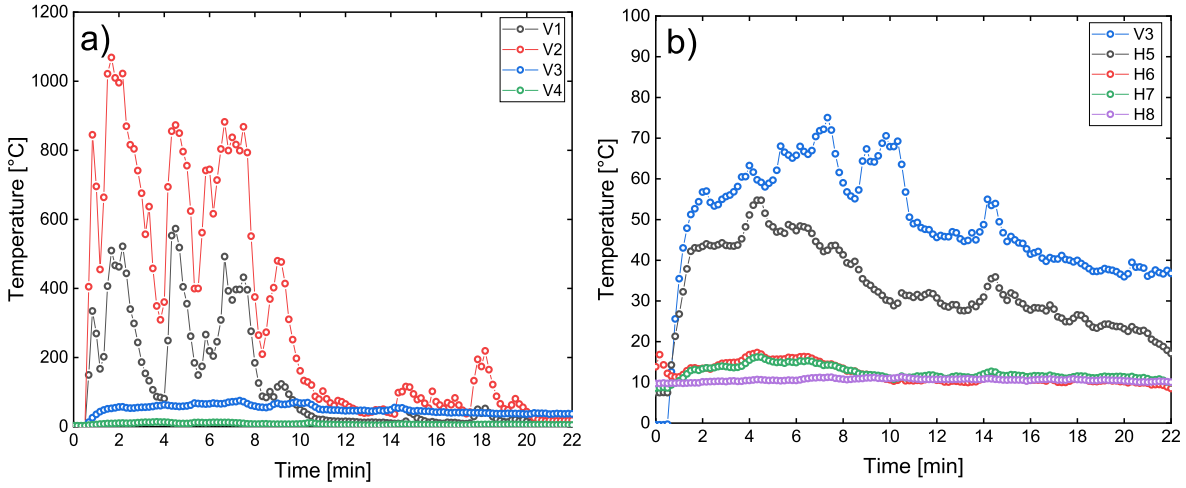

Fig. 10. Time evolution of the vertical a) and horizontal b) temperature profiles measured during Test D.

were monitored and successfully guaranteed along with the whole length of the emptying process. A physic-chemical interpretation of the observed phenomena was provided, paving the way for the design and development of suitable models and procedures for the safe storage and transportation of cryogenic fuels.

Author contributions

Paolo Mocellin: Conceptualization, methodology, software, validation, formal analysis, investigation, data curation, writing—original draft preparation, writing—review and editing, visualization, Gianmaria Pio: Conceptualization, software, formal analysis, data curation, writing—review and editing, visualization, Mattia Carboni: methodology, validation, formal analysis, investigation, writing—original draft preparation, visualization, Francesco Pilo: validation, investigation, resources, Chiara Vianello: resources, writing—review and editing, supervision, funding acquisition, Ernesto Salzano: resources, writing—review and editing, supervision, project administration, funding acquisition.

Declaration of competing interest

The authors declare that they have no known competing financial interests or personal relationships that could have appeared to influence the work reported in this paper.

Data availability

Data will be made available on request.

Appendix A. Supplementary data

Supplementary data to this article can be found online at https://doi.org/10.1016/j.jlp.2023.105123.

References

Aursand, E., Hammer, M., 2018. Predicting triggering and consequence of delayed LNG RPT. J. Loss Prev. Process. Ind. 55, 124–133. https://doi.org/10.1016/j.jlp.2018.06.001.

Babrauskas, V., 1983. Estimating large pool fire burning rates. Fire Technol. 19, 251–261. https://doi.org/10.1007/BF02380810.

Bosen, J.F., 1958. An approximation formula to compute relative humidity from dry bulb and dew point temperatures. Mon. Weather Rev. https://doi.org/10.1175/1520-0493(1958)086<0486:aaftcr>2.0.co;2.

Carboni, M., Pio, G., Mocellin, P., Vianello, C., Maschio, G., Salzano, E., 2022a. Accidental release in the bunkering of LNG: Phenomenological aspects and safety zone. Ocean Eng. 252, 111163. https://doi.org/10.1016/j.oceaneng.2022.111163.

Carboni, M., Pio, G., Mocellin, P., Vianello, C., Maschio, G., Salzano, E., 2022b. On the flash fire of stratified cloud of liquefied natural gas. J. Loss Prev. Process Ind. 75, 104680. https://doi.org/10.1016/j.jlp.2021.104680.

Carboni, M., Pio, G., Vianello, C., Mocellin, P., Maschio, G., Salzano, E., 2022c. Numerical simulation of LNG dispersion in harbours: a comparison of flammable and visible cloud. Chem. Eng. Trans. 90, 355–360. https://doi.org/10.3303/CET2290060.

Carboni, M., Pio, G., Vianello, C., Maschio, G., Salzano, E., 2021. Large eddy simulation for the rapid phase transition of LNG. Saf. Sci. 133, 105001 https://doi.org/10.1016/j.ssci.2020.105001.

Carson, P.A., Mumford, C.J., 2013. Hazardous Chemicals Handbook, Hazardous Chemicals Handbook. https://doi.org/10.1016/C2009-0-24010-4.

Cozzani, V., Gubinelli, G., Salzano, E., 2006. Escalation thresholds in the assessment of domino accidental events. J. Hazard Mater. 129, 1–21. https://doi.org/10.1016/j.jhazmat.2005.08.012.

Esteves, A.S., Reis Parise, J.A., 2013. Mathematical modeling of cryogenic spills onto quiescent sea waters followed by pool fires of liquefied natural gas (LNG). Appl. Therm. Eng. 59, 587–598. https://doi.org/10.1016/j.applthermaleng.2013.06.016.

Guidance on LNG Bunkering to Port Authorities and Administration, 31, 2017. European Maritime Safety Agency, p. 430. January.

George, J.J., Renjith, V.R., George, P., George, A.S., 2019. Application of fuzzy failure mode effect and criticality analysis on unloading facility of LNG terminal. J. Loss Prev. Process Ind. 61, 104–113. https://doi.org/10.1016/j.jlp.2019.06.009.

Gerbec, M., Vidmar, P., Pio, G., Salzano, E., 2021. A comparison of dispersion models for the LNG dispersion at port of Koper, Slovenia. Saf. Sci. 144, 105467 https://doi.org/10.1016/j.ssci.2021.105467.

Hashemi, H., Christensen, J.M., Gersen, S., Levinsky, H., Klippenstein, S.J., Glarborg, P., 2016. High-pressure oxidation of methane. Combust. Flame 172, 349–364. https://doi.org/10.1016/j.combustflame.2016.07.016.

Incropera, F.P., Dewitt, D.P., Bergamm, T.L., Lavine, A.S., 2007. Fundamentals of Heat and Mass Transfer, sixth ed. John Wiley and Sons, Hoboken, USA.

Jeong, B., Park, S., Ha, S., Lee, J. ung, 2020. Safety evaluation on LNG bunkering: to enhance practical establishment of safety zone. Ocean Eng. 216, 107804 https://doi.org/10.1016/j.oceaneng.2020.107804.

Kang, Z., Li, Z., Kang, J., 2022. Risk management framework of LNG offshore transfer and delivery system. Ocean Eng. 266, 113043 https://doi.org/10.1016/j.oceaneng.2022.113043.

Kim, I., Kim, H., Chang, D., Jung, D.H., Sung, H.G., Park, S.K., Choi, B.C., 2021. Emergency evacuation simulation of a floating LNG bunkering terminal considering the interaction between evacuees and CFD data. Saf. Sci. 140, 105297 https://doi.org/10.1016/j.ssci.2021.105297.

Klebanoff, L.E., Pratt, J.W., LaFleur, C.B., 2017. Comparison of the safety-related physical and combustion properties of liquid hydrogen and liquid natural gas in the context of the SF-BREEZE high-speed fuel-cell ferry. Int. J. Hydrogen Energy 42, 757–774. https://doi.org/10.1016/j.ijhydene.2016.11.024.

Koopman, R.P., Ermak, D.L., 2007. Lessons learned from LNG safety research. J. Hazard Mater. 140, 412–428. https://doi.org/10.1016/j.jhazmat.2006.10.042.

Lin, B., Gu, H., Ni, H., Guan, B., Li, Z., Han, D., Gu, C., Shao, C., Huang, Z., Lin, H., 2018. Effect of mixing methane, ethane, propane and ethylene on the soot particle size distribution in a premixed propene flame. Combust. Flame 193, 54–60. https://doi.org/10.1016/j.combustflame.2018.03.002.

Luketa-Hanlin, A., 2006. A review of large-scale LNG spills: experiments and modeling. J. Hazard Mater. 132, 119–140. https://doi.org/10.1016/j.jhazmat.2005.10.008.

Mocellin, P., Vianello, C., Maschio, G., 2018. Facing emerging risks in carbon sequestration networks. A comprehensive source modelling approach. Chem. Eng. 67 https://doi.org/10.3303/CET1867050.

Mokhatab, S., Mak, J.Y., Valappil, J.V., Wood, D.A., 2014. LNG safety and security aspects. In: Mokhatab, S., Mak, J.Y., Valappil, J.V., Wood, D.A. (Eds.), Handbook of Liquefied Natural Gas. Gulf Professional Publishing, Boston, pp. 359–435. https://doi.org/10.1016/B978-0-12-404585-9.00009-X.

Nguyen, V.T., Raghavan, V.S., Quek, R.Y., How, L.B., Yan, D., 2022. Reduced order models for uncertainty quantification of gas plumes from leakages during LNG bunkering. J. Loss Prev. Process Ind. 76, 104724. https://doi.org/10.1016/j.jlp.2022.104724.

Pio, G., Carboni, M., Iannaccone, T., Cozzani, V., Salzano, E., 2019a. Numerical simulation of small-scale pool fires of LNG. J. Loss Prev. Process. Ind. 61, 82–88. https://doi.org/10.1016/j.jlp.2019.06.002.

Pio, G., Carboni, M., Salzano, E., 2019b. Realistic aviation fuel chemistry in computational fluid dynamics. Fuel 254, 115676. https://doi.org/10.1016/j.fuel.2019.115676.

Pio, G., Salzano, E., 2021. Accidental combustion phenomena at cryogenic conditions. Saf. Now. 7 https://doi.org/10.3390/safety7040067.

Pio, G., Salzano, E., 2018. Laminar burning velocity of methane, hydrogen, and their mixtures at extremely low-temperature conditions. Energy Fuel. 32, 8830–8836. https://doi.org/10.1021/acs.energyfuels.8b01796.

Qi, R., Ng, D., Cormier, B.R., Mannan, M.S., 2010. Numerical simulations of LNG vapor dispersion in brayton fire training field tests with ANSYS CFX. J. Hazard Mater. 183, 51–61. https://doi.org/10.1016/j.jhazmat.2010.06.090.

Rana, M.A., Cormier, B.R., Suardin, J.A., Zhang, Y., Mannan, M.S., 2008. Experimental study of effective water spray curtain application in dispersing liquefied natural gas vapor clouds. Process Saf. Prog. 27, 345–353. https://doi.org/10.1002/prs.10275.

Scurlock, R.G., 2015. The future with cryogenic fluid dynamics. Phys. Procedia 67, 20–26. https://doi.org/10.1016/j.phpro.2015.06.005.

Sun, B., Guo, K., Pareek, V.K., 2017. Hazardous consequence dynamic simulation of LNG spill on water for ship-to-ship bunkering. Process Saf. Environ. Protect. 107, 402–413. https://doi.org/10.1016/j.psep.2017.02.024.

Vesovic, V., 2007. The influence of ice formation on vaporization of LNG on water surfaces. J. Hazard Mater. 140, 518–526. https://doi.org/10.1016/j.jhazmat.2006.10.039.

Vianello, C., Carboni, M., Mazzaro, M., Mocellin, P., Pilo, F., Pio, G., Salzano, E., 2020. Hydrogen Refueling Stations: Prevention and Scenario Management. Large Scale Experimental Investigation of Hydrogen Jet-fires. Chem. Eng. Trans. 82, 247–252. https://doi.org/10.3303/CET2082042.

Withers, M.R., Malina, R., Gilmore, C.K., Gibbs, J.M., Trigg, C., Wolfe, P.J., Trivedi, P., Barrett, S.R.H., 2014. Economic and environmental assessment of liquefied natural gas as a supplemental aircraft fuel. Prog. Aero. Sci. 66, 17–36. https://doi.org/10.1016/j.paerosci.2013.12.002.

Xiao, X.K., Kuang, K.Q., Liang, T.S., Tang, H.D., Liao, G.X., Yuen, K.K.R., 2011. Study on flame expansion phenomenon in pool fire extinguished by water mist. Procedia Eng. 11, 550–559. https://doi.org/10.1016/j.proeng.2011.04.695.